Eur. Phys. J. B **19**, 491–499 (2001)

THE EUROPEAN PHYSICAL JOURNAL B

EDP Sciences

The influence of the dynamics of ionic multiplets onto electronic transport properties of heavy-fermion systems: a semi-phenomenological approach

F.B. Anders[1,a] and M. Huth[2]

[1] Institut für Festkörperphysik, Technische Universität Darmstadt, 64283 Darmstadt, Germany
[2] Institut für Physik, Johannes Gutenberg–Universität Mainz, 55099 Mainz, Germany

Received 30 June 2000 and Received in final form 15 December 2000

Abstract. We present calculations of the electronic transport properties of heavy-fermion systems within a semi-phenomenological approach to the dynamical mean field theory. In this approach the dynamics of the Hund's rules $4f(5f)$-ionic multiplet split in a crystalline environment is taken into account. Within the scope of this calculation we use the linear response theory to reproduce qualitative features of the temperature–dependent resistivity and hall conductivity, the magneto-resistivity and the thermoelectric power typical for heavy-fermion systems. The model calculations are directly compared with experimental results on $CeCu_2Si_2$.

PACS. 71.27.+a Strongly correlated electron systems; heavy fermions – 72.10.-d Theory of electronic transport; scattering mechanisms – 72.15.Qm Scattering mechanisms and Kondo effect – 73.50.Jt Galvanomagnetic and other magnetotransport effects (including thermomagnetic effects)

1 Introduction

Strong electronic correlations are the crucial aspect of the physics of heavy-fermion systems [1]. The local Coulomb repulsion on the $4f$ or $5f$ lattice sites causes the atomic part of the Hamiltonian to be of non-bilinear form. Consequently, the hybridization of the local f-electrons with the itinerant states cannot be treated in a conventional Feynman perturbation theory [2]. Several different theoretical concepts have been developed during the last 10 to 15 years to treat this problem. These are rooted in the somewhat simpler Kondo problem or single–impurity problem that is now well–understood (for recent reviews see [3]). If the f-moments are localized on a regular lattice the problem is rendered even more difficult, since the mechanism of coherent scattering for temperatures much below the Kondo energy scale T_K has to be introduced in the theory adequately in order to describe the observed coherence effects in the electronic transport properties.

A fully self-consistent microscopic theory for the Anderson-lattice model developed in this context is based on the the mapping of the lattice onto an effective impurity [4,5] embedded in a bath of conduction electrons. This theory becomes exact in infinite dimensions and incorporates all local interactions in finite spatial dimension. In the literature it is referred to as dynamical mean field theory (DMFT). The DMFT is able to reproduce the basic aspects of coherent scattering at low temperatures, such as a quadratic dependence of the resistivity on temperature. As far as transport is concerned, the average T-matrix approximation was applied in the 1980s to understand the fundamental transport properties [6–9]. It was shown that this approximation captures the conduction electron lifetime, the relevant quantity for transport calculations, surprisingly well as can be seen by a comparison of the single impurity and the lattice f-self-energy [10].

Nevertheless, in heavy-fermion materials [1] a simple periodic Anderson model (PAM), with single N-fold degenerate ionic ground-state, cannot explain the rich variety of transport measurements over the whole accessible temperature range. The additional maxima found experimentally in the electrical resistivity, the thermoelectric power and also in the specific heat are related to higher crystal-electric-field (CEF) levels and have been used to propose CEF-level schemes for many different heavy-fermion compounds. Many theoretical attempts have been put forward to include CEF-effects in a many-body description of heavy-fermion materials [11]. For magnetic impurities high temperature spin-disorder resistance calculations [12] were extended to describe the anisotropic transport properties of $CePt_2Si_2$ in third order perturbation theory [13]. Usually, the dynamics of all ionic levels resulting from the Hund's rules multiplet, which has been split in crystalline environment, is not fully accounted for: lattice coherence effects and important local quantum-fluctuations are neglected. Anderson lattice approaches

[a] e-mail: frithjof@fkp.tu-darmstadt.de

including CEF-effects exist only within the slave boson mean field theory [14]. Additionally, the low temperature scale T^* will reflect higher excited multiplets due to the remaining quantum fluctuations in the ground state.

Given the complicated numerical procedures for solving the dynamical mean field theory [15,16], we consider a simplified approach including the essential aspects of the Kondo lattice to be very helpful. For that reason a semi-phenomenological description of crystal field effects in Kondo lattices based on the DMFT was developed which is applicable to any local approximation [17]. This approach is able to give further insight into the respective influences of the different relevant energy scales in heavy-fermion systems on the measured electronic transport quantities. The resummation of the complex local scattering events involving CEF-levels of the $4f(5f)$ electrons yields a rather simple result in agreement with Matthiessen's law and our physical intuition. To begin with, the DMFT is briefly reviewed starting with the formulation of the Anderson–lattice Hamiltonian in a generalized form based on the irreducible representations of the point group of the crystal. The aim of this paper is to present a semi-phenomenological approach for the study of CEF effects in lattice calculations. We show explicitly how lattice coherence is restored at low temperature which could not be obtained by previous single impurity approaches. The results are exemplified for a Kramers ion in a tetragonal crystal field. The derivation of the conduction electron Green function is based on a semi-phenomenological approximation to the local excitation spectrum. In order to calculate the dc and the Hall conductivity we apply recent results based on linear response theory [4,18]. Using the relationship between the conduction electron Green function and the transport relaxation time the thermopower is obtained within the linearized Boltzmann theory. Finally, the calculations are complemented by a comparison with experimental results.

2 Description of the model

The concept of the approximate treatment of the Anderson lattice for the transport properties was introduced by Grewe and Pruschke [6], used by Cox and Grewe [8] and extended to magneto-transport by Lorek, Anders and Grewe [9]. It is based on the local approximation and uses the local T-matrix describing a single scattering event of a conduction electron off the f-electrons. The lattice coherence is taken into account by resummation of an infinite number of those individual scattering events. In the next section this approximate treatment will be briefly reviewed and completed by a consideration of the crystal field level scheme. The transport coefficients are calculated using linear response theory and the transport integral method of the linearized Boltzmann theory.

2.1 The DMFT including the crystal field

The starting point of our derivation is given by the Anderson-lattice Hamiltonian. A spin-degenerate conduction electron band couples to localized crystal field-split ionic states by means of hybridization matrix elements. Fluctuations on the ionic sites are limited to those between singly occupied or empty states, *i.e.* the repulsive interaction on the ionic sites is assumed to be infinite. The Hamiltonian is given by the following expression

$$\mathcal{H} = \sum_{\mathbf{k}\sigma} \epsilon_{\mathbf{k}\sigma} c^+_{\mathbf{k}\sigma} c_{\mathbf{k}\sigma} + \sum_{\nu,\Gamma\alpha} E_{\Gamma\alpha} X^{\nu}_{\Gamma\alpha,\Gamma\alpha} + \sum_{\nu,\mathbf{k}\sigma,\Gamma\alpha} \left[V_{0,\Gamma\alpha}(\mathbf{k}\sigma) \mathrm{e}^{\mathrm{i}\mathbf{k}\cdot\mathbf{R}_\nu} c^+_{\mathbf{k}\sigma} X^{\nu}_{0,\Gamma\alpha} + \text{h.c.} \right]. \quad (1)$$

The first part describes the kinetic energy of the uncorrelated band electrons. The energy of occupied local states is given by the second part. Finally, the hybridization between local and itinerant states is formulated by the third part of the Hamiltonian. Γ denotes an irreducible representation of the point group of the crystal, α a state of that representation and $X^{\nu}_{\Gamma'\alpha',\Gamma\alpha} = |\Gamma'\alpha'^{\nu}\rangle\langle\Gamma\alpha^{\nu}|$ the Hubbard projection operator at the site ν.

In the periodic Anderson model the T–matrix $T_{\mathbf{k}\sigma}(z)$ is related to the local Green function $F_{\Gamma\alpha,\Gamma\alpha}(\mathbf{k},z)$ in the following way [19,20]

$$T_{\mathbf{k}\sigma}(z) = \sum_{\Gamma'\alpha',\Gamma\alpha} V_{0,\Gamma\alpha}(\mathbf{k}\sigma) F_{\Gamma'\alpha',\Gamma\alpha}(\mathbf{k},z) V^*_{\Gamma'\alpha',0}(\mathbf{k}\sigma) \quad (2)$$

which can be written in a more compact form by using a matrix formalism

$$T_{\mathbf{k}\sigma}(z) = \mathbf{V}^t(\mathbf{k}\sigma) \underline{\underline{F}}(\mathbf{k},z) \mathbf{V}(\mathbf{k}\sigma) \quad (3)$$

introducing the hybridization vector $\mathbf{V}^t(\mathbf{k}\sigma)$ and the Green function matrix $\underline{\underline{F}}(\mathbf{k},z)$

$$\mathbf{V}^t(\mathbf{k}\sigma) \equiv (V^*_{\Gamma_1\alpha_1,0}(\mathbf{k}\sigma), \ldots, V^*_{\Gamma_n\alpha_n,0}(\mathbf{k}\sigma)) \quad (4)$$

$$\underline{\underline{F}}(\mathbf{k},z)\big|_{\Gamma'\alpha',\Gamma\alpha} \equiv F_{\Gamma'\alpha',\Gamma\alpha}(\mathbf{k},z) \equiv \frac{1}{N} \sum_{\nu} \mathrm{e}^{\mathrm{i}\mathbf{k}\,\mathbf{R}_\nu} \langle\langle X^{\nu}_{0,\Gamma'\alpha'}(\tau) X^{0}_{\Gamma\alpha,0} \rangle\rangle. \quad (5)$$

(N: number of lattice sites).
With the exact equation of motion [19] for the conduction electron Green function

$$G_{\mathbf{k}\sigma}(z) = G^{(0)}_{\mathbf{k}\sigma} + G^{(0)}_{\mathbf{k}\sigma}(z) T_{\mathbf{k}\sigma}(z) G^{(0)}_{\mathbf{k}\sigma}(z) \equiv \frac{1}{z - \epsilon_{\mathbf{k}\sigma} - \Sigma_{\mathbf{k}\sigma}(z)} \quad (6)$$

we obtain the following expression for the band self–energy [20]:

$$\Sigma_{\mathbf{k}\sigma}(z) = \frac{\mathbf{V}^t(\mathbf{k}\sigma) \underline{\underline{F}}(\mathbf{k},z) \mathbf{V}(\mathbf{k}\sigma)}{1 + G^{(0)}_{\mathbf{k}\sigma} \mathbf{V}^t(\mathbf{k}\sigma) \underline{\underline{F}}(\mathbf{k},z) \mathbf{V}(\mathbf{k}\sigma)} \quad (7)$$

$$= \mathbf{V}^t(\mathbf{k}\sigma) \underline{\underline{F}}(\mathbf{k},z) \frac{1}{\underline{\underline{1}} + \underline{\underline{\Delta}}(\mathbf{k}\sigma,z) \underline{\underline{F}}(\mathbf{k},z)} \mathbf{V}(\mathbf{k}\sigma)$$

$$\underline{\underline{\Delta}}(\mathbf{k}\sigma,z) \equiv \mathbf{V}(\mathbf{k}\sigma) G^{(0)}_{\mathbf{k}\sigma} \mathbf{V}^t(\mathbf{k}\sigma). \quad (8)$$

The aim of the DMFT is to obtain an approximate expression for the T-matrix and local Green function [4,5] which takes into account almost all local correlations, since they are responsible for the strong renormalization of the quasi-particles. In the lattice the formal delocalization of a local f-electron *via* hybridization into a band electron state may be followed by additional scattering events on different lattice sites before the re-localization into any local state takes place. The DMFT for the Anderson lattice [4,5,21] maps this problem onto an effective f-site sitting in an fictitious conduction band bath. Since the original conduction bands are non-interacting, equations (3, 7) are exact: in contrast to the situation for the Hubbard-model, only the f-self-energy is set to be local. The k-dependent f-Green function has matrix character in the (Γ, α) space of interest and reads [20]

$$\underline{\underline{F}}(\mathbf{k}, z) = \frac{1}{\underline{\underline{\tilde{F}}}(z)^{-1} - \left(\sum_{\sigma} \underline{\underline{\Delta}}(\mathbf{k}\sigma, z) - \underline{\underline{\tilde{\Delta}}}(z) \right)}, \qquad (9)$$

where the definition (8) has been used. $\underline{\underline{\tilde{\Delta}}}(z)$ is the matrix of the dynamical mean field components of the effective site. This leads to the DMFT self-consistency condition

$$\sum_{\mathbf{k}} \frac{1}{\underline{1} - \underline{\underline{\tilde{F}}}(z) \left(\sum_{\sigma} \underline{\underline{\Delta}}(\mathbf{k}\sigma, z) - \underline{\underline{\tilde{\Delta}}}(z) \right)} = 1, \qquad (10)$$

where $\underline{\underline{\tilde{F}}}(z)$ is the local f-Green function of the effective site [20,21].

Inserting the DMFT approximation (9) into the exact equation (7) yields the following expression for the band self-energy that is central for the discussion of the transport properties:

$$\Sigma_{\mathbf{k}\sigma}(z) = \mathbf{V}^t(\mathbf{k}\sigma) \frac{1}{\underline{\underline{\tilde{F}}}(z)^{-1} + \underline{\underline{\tilde{\Delta}}}(z) - \underline{\underline{\Delta}}(\mathbf{k} - \sigma, z)} \mathbf{V}(\mathbf{k}\sigma). \qquad (11)$$

Note the fact that even a local approximation like the DMFT can include the leading anisotropies in the conduction electron self-energy by using an angular dependent hybridization vector $\mathbf{V}(\mathbf{k}\sigma)$. The term $-\underline{\underline{\Delta}}(\mathbf{k}-\sigma, z)$ in equation (11) is projected away by $\mathbf{V}(\mathbf{k}\sigma)$ because of spin conservation if Γ are elements of a double group [22]. A similar approach for the Hubbard model has been used to combine local density approximations and DMFT [23,24].

2.2 Example: three doublets – Kramers ion in tetragonal crystal field

For further discussion we consider the level scheme of a Kramers ion (*e.g.* Ce^{3+}) in a tetragonal crystal field. In this case the Hund ground state multiplet $J = 5/2$ splits into three magnetic doublets. The hybridization is assumed to be spin–conserving without $\mathbf{k}$–dependence. Since the local pseudo–spin is a good quantum number, the hybridization couples only to one crystal field eigenstate in either of the three doublets for a given band electron spin direction. Consequently, the hybridization matrix is block diagonal and the 6×6–matrix decomposes into two 3×3–matrices with vanishing matrix elements in the upper/lower block matrix for local down/up spin direction. Since the band electron Green function has to be diagonal in the spin the same structure is given for the matrix $\underline{\underline{\Delta}}(\mathbf{k}\sigma, z)$ resulting again in a block diagonal form of $\underline{\underline{\tilde{\Delta}}}(z)$. Finally, the effective site Green function matrix is diagonal due to the local hybridization. As a consequence, the band self–energy decomposes for a given band electron spin into a sum of the self–energy contributions for the three doublet states

$$\Sigma_{\mathbf{k}\sigma}(z) = \sum_{j=1}^{3} \frac{V_j^2 \tilde{F}_j(z)}{1 + \tilde{F}_j(z) \tilde{\Lambda}_{jj}(z)} \,. \qquad (12)$$

A crossover to the single impurity Kondo effect can be accomplished by furnishing the scattering matrix with a pre-factor c_{imp} that represents the concentration of the magnetic impurities

$$V_j^2 \tilde{F}_j(z) \quad \rightarrow \quad c_{\mathrm{imp}} V_j^2 \tilde{F}_j(z). \qquad (13)$$

After the expansion of the band self energy in equation (12) with respect to the small quantity c_{imp} the following result is obtained

$$\Sigma_{\mathbf{k}\sigma}(z) = c_{\mathrm{imp}} \left(\sum_{j=1}^{3} V_j^2 \tilde{F}_j(z) \right). \qquad (14)$$

2.3 Approximate treatment

Pruschke *et al.* [10] have recently shown that the f-self energy of the periodic Anderson model calculated at $T = 0$ with DMRG+NRG preserves the Fermi-liquid properties known from the SIAM and differs only by the low-energy scale for a given set of parameters. The information about possible hybridization gaps are contained in the media $\Lambda_j(z)$ and local Green function $\tilde{F}_j(z)$. The dominating influence on the transport properties is exerted by the many particle resonance structure near the Fermi surface. Since the low temperature scale is set by the experiment as an input parameter, and $\tilde{F}_j^{-1}(z) + \Lambda_j(z)$ describes a Fermi-liquid, it is justified for our purpose to approximate the local Green functions by a Lorentzian curve

$$\tilde{F}_j(\omega) = \frac{a(T/T_{\mathrm{K}j})}{\omega - \eta_j - \mathrm{i}\gamma_j} \qquad (15)$$

in order to reproduce the correct form of $\Sigma_{\mathbf{k}\sigma}(z)$. The low energy scale T_{K0} determines both the width $\gamma = \pi/(2N+1) k_{\mathrm{B}} T_{\mathrm{K0}}$ and the position $\eta = k_{\mathrm{B}} T_{\mathrm{K0}}$ of the main resonance. The exact position of the resonance should be in accordance with Friedel's sum rule. The position and width of the N_j degenerated excited crystal field levels

are given by $\Delta_{0j} + T_{\mathrm{K}0}$ and $\gamma_j = \pi/(2N_j+1)k_{\mathrm{B}}T_{\mathrm{K}_j}$ (Δ_{0j}: crystal-field splitting), respectively.

As is well-known from renormalization group theory the low temperature properties of a Kondo system are dominated by the low temperature energy scale T_{K}. The argument of the temperature–dependent function $a(T/T_{\mathrm{K}j})$ is therefore given by a relative temperature for the respective crystal field levels. All calculations performed in the following sections are based on the following temperature dependence

$$a(T/T_{\mathrm{K}j}) = \begin{cases} \frac{\gamma_i}{\tilde{\Lambda}_j}(1 - b(T/T_{\mathrm{K}j})^2) : \; T \ll T_{\mathrm{K}j} \\ a_0(1 - \frac{\ln(T/T_{\mathrm{K}j})}{\sqrt{(\ln(T/T_{\mathrm{K}j}))^2 + \pi^2 S_j(S_j+1)}}) : T \geq T_{\mathrm{K}j}. \end{cases} \tag{16}$$

The quadratic temperature dependence for $T \ll T_{\mathrm{K}j}$ is motivated by the Fermi-liquid character of the quasiparticle excitations at low temperature. The pre-factor $\gamma_i/\tilde{\Lambda}_j$ is a consequence of the limiting behaviour of the local density of states for $T \to 0$ [25]

$$N_j(\omega) = -\frac{1}{\pi}\mathrm{Im}\tilde{F}_j(\omega - \mathrm{i}\delta) = \frac{\gamma_j^2}{\pi\tilde{\Lambda}_j[(\omega - \eta_j)^2 + \gamma_j^2]} \cdot \tag{17}$$

It reflects the many body nature of the resonance: only the fraction $\sum_j \tilde{\gamma}_j/\Lambda_j < 1$ of f-electrons participates in the scattering. In the temperature region $T \geq T_{\mathrm{K}j}$ we use the results of the parquet diagram expansion of the Nagaoka–Suhl equations for the sd–model [26]. The parameters a_0 and b are fixed by adjusting equation (16) to the temperature dependence of the resonance height within the PNCA procedure ($N_j = 2$). In the region between the low temperature and high temperature limiting cases a polynomial fit based again on the PNCA results [27] is used.

The influence of a magnetic field on the transport properties can be accounted for by introducing a Kondo field $B_{\mathrm{K}j}$ that is given by the following relation for the respective crystal field level

$$k_{\mathrm{B}}T_{\mathrm{K}j} = \mu_j B_{\mathrm{K}j}. \tag{18}$$

The argument of the function $a(x_j)$ is now given by a generalized form that includes temperature and field on an equal base and guarantees an isotropic field dependence in accordance with the assumed **k**–independent hybridization

$$x_j = \sqrt{\left(\frac{T}{T_{\mathrm{K}j}}\right)^2 + \left(\frac{B}{B_{\mathrm{K}j}}\right)^2}. \tag{19}$$

Equation (19) is only a natural way of parameterization of the decrease of the quasi-particle spectral weight with temperature or magnetic field and does not reflect a scaling law in the strict sense. Within the Lorentz approximation of the effective site Green function a Zeeman splitting of the crystal field states has to be taken into account

$$\tilde{F}_j(\omega) = \frac{a(x_j)}{\omega - (\eta_j + \mu_j B) - \mathrm{i}\gamma_j} \cdot \tag{20}$$

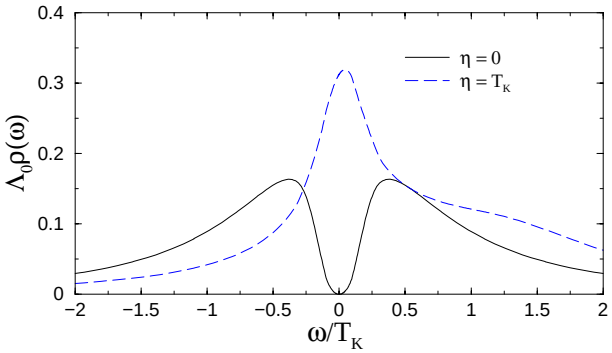

Fig. 1. The local f-Green function of the lattice obtained with *ansatz* (15) and equation (9) for one CEF multiplet with $\eta = 0$ and $\eta_0 = T_{\mathrm{K}}$. $\eta = 0$ corresponds to the Kondo-Insulator regime with a clearly visible hybridization gap, and $\eta = T_{\mathrm{K}}$ simulates the strongly asymmetic metallic regime, where the gap is completely smeared out. Parameters: $\Lambda = 1163$ K, $T_{\mathrm{K}} = 9$ K, $\gamma = 0.01$, $T = 0$.

To demonstrate the variety of different lattice parameters, which can be mimiced using the ATA *ansatz*, we use equation (15) for two different parameters of η in combination with equation (9) to calculate the local f-Green function of the lattice for a single CEF multiplet, depicted in Figure 1. $\eta = 0$ describes the Kondo insulator scenario, and $\eta = T_{\mathrm{K}}$ the metallic situation. Clearly visible is the hybridization gap for $\eta = 0$ which is absent in the asymmetic case.

Nevertheless, in the paramagnetic phase of the model we expect that there is only one low temperature energy scale, the lattice Kondo temperature, which we set equal to $T_{\mathrm{K}0}$. There are strong hints in recent DMFT(QMC) calculations that by reduction of the number of conduction electrons per site, the PAM has two low temperature scales: a scale which tends to coincide with the SIAM T_{K} and a low temperature scale T_0 which describes the coherent regime [28]. The HF-compounds, however, seem to be closer to the opposite limit, since the number of electrons from the conduction bands outnumber usually the number of f-electrons in these complicated compounds [29]. Moreover, experiments on $\mathrm{La}_x\mathrm{Ce}_{1-x}\mathrm{Cu}_6$ [30] reveal that the change of the low energy scale can be understood solely in terms of the La-contraction in this compound. Whether the starting point (1) is incomplete, or spatial fluctuations ignored in any local approximation are more important than anticipated, is not clear at the moment. Additional low energy scales like the Néel temperature [31] or the superconducting T_{c} [32] can be calculated by analysing the residual quasi-particle interactions [15,17,33].

2.4 Relationship to transport theory

Based on the results of the preceding sections the band electron Green–function is now used to give explicit expressions for different electronic transport properties. It has been shown, that the f-electrons do not contribute

to the transport in case of **k**-independent hybridisation due to cancelling of all vertex corrections [7–9,20,34]. The spin-dependent transport relaxation time $\tau_\sigma(\omega)$ is given by [8,35]

$$\tau_\sigma(\omega) = \frac{d}{h v_{\rm F}^2 N_{\rm F}} \frac{1}{N} \sum_{\mathbf{k}} \left(\frac{\partial \epsilon_{\mathbf{k}}}{\partial k_x} \right)^2 [{\rm Im} G_\sigma(\mathbf{k}, \omega - {\rm i}\delta)]^2 {\rm d}\epsilon, \tag{21}$$

where $v_{\rm F}$ is the averaged Fermi-velocity, $N_{\rm F}$ the density of states at the chemical potential and d the dimension. It can be shown that in the Fermi-liquid regime for $T \to 0$ the well known result

$$\tau_\sigma(z = x - {\rm i}\delta) \sim \frac{\hbar}{2{\rm Im}\Sigma_\sigma(x - {\rm i}\delta)} \tag{22}$$

is recovered. Summing the spin–dependent relaxation times over the spin index leads to the total transport relaxation time

$$\tau(z = x - {\rm i}\delta) = \sum_\sigma \tau_\sigma(z = x - {\rm i}\delta). \tag{23}$$

This can be used to determine several transport quantities like the specific resistivity ρ, the thermopower S and the Hall coefficient $R_{\rm H}$ based on the transport integrals L_{mr} derived from a linearized Boltzmann transport theory [36]:

$$L_{mr} = \int_{-\infty}^{\infty} \left(-\frac{\partial f}{\partial \omega} \right) \tau^m(\omega) (\hbar\omega)^r \, {\rm d}\omega \tag{24}$$

$$\rho = \frac{4\pi}{\omega_p^2} \frac{1}{L_{10}} \tag{25}$$

$$S = -\frac{1}{|e|T} \frac{L_{11}}{L_{10}} \tag{26}$$

$$R_{\rm H} = -\frac{2}{ne} \frac{L_{20}}{L_{10}^2} \tag{27}$$

where $\omega_{\rm p}$ is the plasma frequency and n the conduction electron density. For a quadratic dispersion we obtain $\omega_{\rm p}^2/(4\pi) = ne^2/m^*$. It follows immediately from the analytic form of (27) that the the Hall-coefficient must be negative at all temperatures within this approximation. This is in contrast to many experimental findings. Vorunganti *et al.* recently showed how to go beyond the Boltzmann approach for correlated electrons. They derived the Hall-conductivity within linear response theory [18]

$$\sigma_{xyz}^H = -\frac{n|e|^3}{3\hbar^2\pi} \int_{-\infty}^{\infty} {\rm d}\omega \left(-\frac{\partial f(\omega)}{\partial \omega} \right) \times \frac{1}{N} \sum_{\mathbf{k}\sigma} \left(\frac{\partial \epsilon_{\mathbf{k}}}{\partial k_x} \right)^2 \frac{\partial^2 \epsilon_{\mathbf{k}}}{\partial k_y^2} [{\rm Im} G_\sigma(\epsilon_{\mathbf{k}}, \omega - {\rm i}\delta)]^3 \tag{28}$$

and

$$R_{\rm H} = \rho^2 \sigma_{xyz}^H \tag{29}$$

which has been successfully applied to the Hubbard-Model in large dimensions [4]. For a simple-cubic band-structure $\epsilon_{\mathbf{k}} = -2t \sum_{i=1}^3 \cos(k_i a)$ and $\rho_0(\epsilon)$ being the DOS of the non-interacting electron gas, the following formulas have been derived by Pruschke *et al.* [4]

$$I_{dc} = 2t^2 \sum_\sigma \int_{-\infty}^{\infty} {\rm d}\omega \left(-\frac{\partial f(\omega)}{\partial \omega} \right) \times \int_{-\infty}^{\infty} {\rm d}\epsilon \rho_0(\epsilon) [{\rm Im} G_\sigma(\epsilon, \omega - {\rm i}\delta)]^2 \tag{30}$$

$$I_{\rm H} = \frac{4t^2}{3d} \sum_\sigma \int_{-\infty}^{\infty} {\rm d}\omega \left(-\frac{\partial f(\omega)}{\partial \omega} \right) \times \int_{-\infty}^{\infty} {\rm d}\epsilon \rho_0(\epsilon) e [{\rm Im} G_\sigma(\epsilon, \omega - {\rm i}\delta)]^3 \tag{31}$$

$$\rho^{-1} = \frac{na^3e^2}{2\hbar a} I_{dc} \tag{32}$$

$$R_{\rm H} = \frac{1}{|e|n} \frac{I_{\rm H}}{I_{dc}^2} \tag{33}$$

I_{dc} and $I_{\rm H}$ are dimensionless quantities. Hence, the absolute units for the resistivity and the Hall coefficient can be obtained by the carrier concentration n and the length of the unit cell a.

Since we do not solve the DMFT equation (10) self-consistently within our semi-phenomenological approach, we use $\tilde{\Lambda}_{jj}(\omega + {\rm i}\delta) \approx -{\rm i}\pi V_j^2 \rho(\epsilon_{\rm F}) = -{\rm i}\Delta_j$, where Δ_j is the Anderson width for the CEF state j. Consequently, within the three doublet scenario, the calculation of the transport quantities in the subsequent section is based upon the following self–energy:

$$\Sigma_\sigma(z = \omega \pm {\rm i}\delta) = \sum_{j=1}^3 \frac{V_j^2 \tilde{F}_j(\omega \pm {\rm i}\delta)}{1 \mp {\rm i}\tilde{F}_j(\omega \pm {\rm i}\delta)\Delta_j} \cdot \tag{34}$$

In the low temperature region equation (34) reflects Matthiessen's law according to which the resistivity is proportional to the sum of the inverse relaxation times.

3 Comparison with experimental results

In the following we compare the results of the model calculation with the transport properties of the heavy–fermion system $CeCu_2Si_2$. In $CeCu_2Si_2$ the crystal–field splitting between the low lying Kramers doublet and two energetically–degenerated excited doublets is much larger than the low temperature energy scale $T_{\rm K0}$ [37]. Possible magnetic exchange scattering contributions to the resistivity are neglected. Unlike the crystal–field splittings Δ_{0j} and the Kondo temperature $T_{\rm K0}$, the Kondo temperatures of the excited doublets $T_{{\rm K}j}$ and the corresponding Anderson widths of the respective levels Δ_j are not known. In order to derive Anderson widths which are consistent with the fixed Kondo temperature of the ground doublet and the Kondo temperatures of the excited doublets the so called "poor man's" scaling result [3]

$$k_{\rm B} T_{\rm K} = \sqrt{D\Delta} \exp\left(-\pi |\epsilon_f| / 2\Delta\right) \tag{35}$$

is used with fixed values for the cutoff parameter $D = 2.5$ eV and the position of the localized f–level $\epsilon_f = -2$ eV (typical values). For simplicity we assume equal Kondo–temperatures $T_{K1} = T_{K2}$ for the energetically–degenerated excited two doublets. The Kondo temperature for the ground doublet state $|0\rangle = -\eta|\pm 5/2\rangle + \sqrt{1-\eta^2}|\mp 3/2\rangle$ is set to 9 K according to reference [1] with $\eta = 0.467$ [37]. The crystal–field splittings are known from inelastic neutron scattering to be $\Delta_{01} = \Delta_{02} = 350$ K for both excited levels $|1\rangle = \sqrt{1-\eta^2}|\pm 5/2\rangle + \eta|\mp 3/2\rangle$ and $|2\rangle = |\pm 1/2\rangle$. In cubic symmetry, with $\eta = \sqrt{1/6} = 0.408$, $|1\rangle$ and $|2\rangle$ would form the Γ_8 quartet. We assume a number density of charge $n = 2.5 \times 10^{22}$ cm^{-3} and one electron per unit cell ($na^3 = 1$); hence $a = 3.4 \times 10^{-8}$ cm. Additionally, we neglect the temperature dependence of the Lorentzian widths γ_i in order to maintain the lowest possible set of parameters. The maxima due to higher crystal–field states will therefore appear more pronounced. The following paragraph will show that the simplifying assumption of an isotropic band structure results in quantitative differences between the calculated and experimentally determined higher–order transport coefficients. Nevertheless, the aim of the present calculation is to give a qualitative correspondence.

In Figure 2 a representative temperature-dependent resistivity curve is contrasted with the model calculation for different Kondo temperatures of the excited doublets. In order to facilitate a comparison with the experimental data a residual resistivity of 20 $\mu\Omega$ cm and the phononic resistivity contribution of a $LaCu_2Si_2$ reference–sample [38] was added to the calculated curves. The qualitative correspondence is best for an excited doublet Kondo temperature of about 120 K as far as the position of the high temperature maximum in the resistivity is concerned. Interesting enough, the width of the crystal–field transition observed by Goremychkin *et al.* [37] is about 100 K due to the strong interactions of the f–electrons with the conduction band in good correspondence with our estimate of the Kondo temperature of the excited doublets. The low temperature maximum is more pronounced in the calculation. This is also true for $CeCu_2Si_2$ samples with lower residual resistivity. The resistivity data of reference [38] was primarily taken since this represents a common feature of disordered Kondo lattices. With increasing disorder in the system a distribution of hybridization strengths and positions of the local f–states is generated that cause a much broader distribution of Kondo temperatures according to the exponential dependence in equation (35). A distribution of Kondo temperatures might cause a significant rounding of the low temperature maximum. Due to electronic correlations the disorder–induced scattering rates grow faster than in uncorrelated systems. As a consequence, the coherent scattering part is reduced and the influence of disorder cannot be accounted for by a simple increase in the residual resistivity [39]. As shown in the inset of Figure 2b the low temperature part of the calculated resistivity follows a quadratic temperature dependence, as is expected in the Fermi–liquid regime. The low temperature resistivity of reference [38] reveals an interesting deviation from the quadratic behavior following a linear dependence. This might be caused by a a quantum critical point in $CeCu_2Si_2$ as recently discussed by Steglich *et al.* [40]. Based on the fixed parameter set with $T_{K1} = T_{K2} = 120$ K, Figures 3–5 show a comparison of several additional transport quantities as function of temperature. The top part represents experimental data from various references whereas the bottom part shows the calculated quantities.

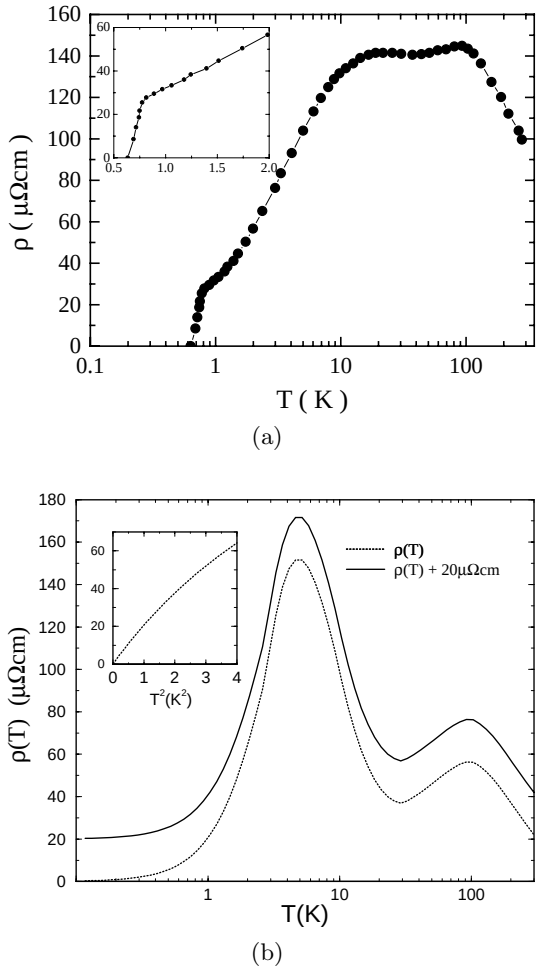

Fig. 2. Comparison of the temperature dependent resistivity of $CeCu_2Si_2$ (a) with the model calculation (b). The inset in (b) shows the calculated resistivity without residual resistivity and phonon contribution as a function of T^2. The resistivity data is taken from reference [38].

The calculated magneto-resistivity is in good correspondence with the experimental data as shown in Figure 3. Even the shallow maximum around 30 K caused by the excited crystal-field states is reproduced. Quantitatively the magneto-resistivity at low temperatures reaches 800% in the calculation (with 20 $\mu\Omega$ cm residual resistivity) whereas the experimental value is 10%. The reason for the reduced magnetoresistivity in the experimental data might also be traced back to the same influence of disorder on the coherent scattering part in the resistivity.

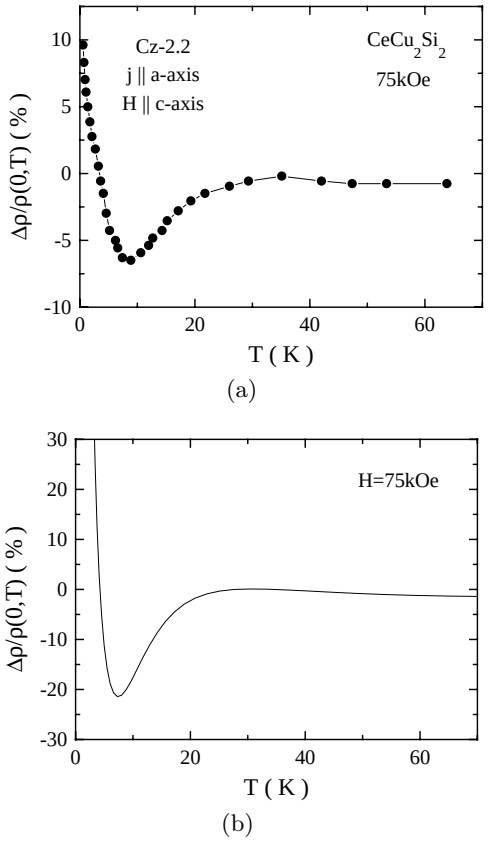

Fig. 3. Comparison of the temperature dependence of the magneto-resistivity of $CeCu_2Si_2$ [38] (a) with the model calculations (b).

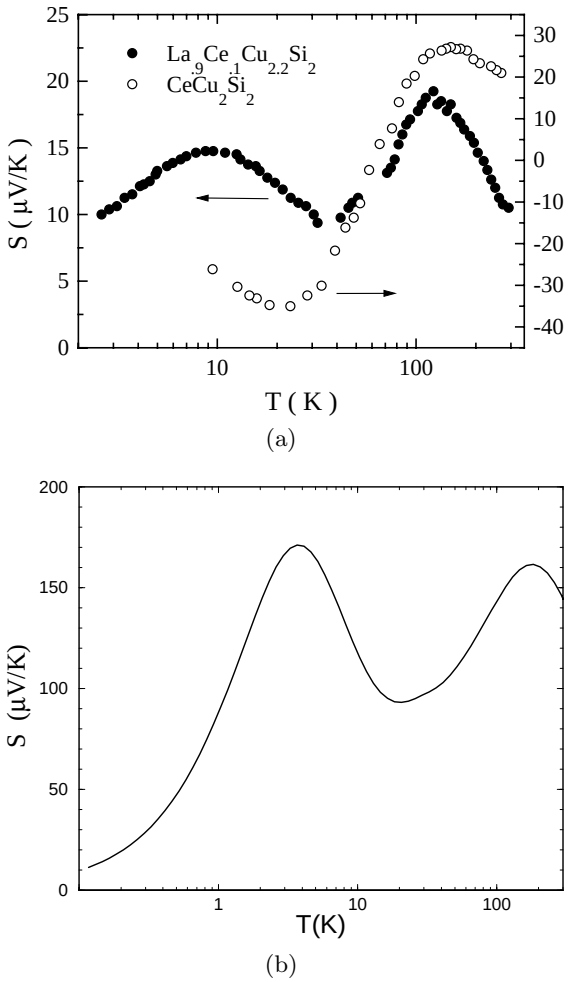

Fig. 4. Comparison of the temperature dependence of the thermoelectric power of $CeCu_2Si_2$ [44] and $La_{0.9}Ce_{0.1}Cu_{2.2}Si_2$ [40] (a) with the model calculations (b).

Furthermore the calculation does not include possible band–structure effects.

According to the calculation the Seebeck coefficient shows no sign-reversal; this is in contradiction to the experimental result. Furthermore, the low temperature maximum does not appear in the experimental data. The absolute values in the calculation are significantly higher. This could be attributed to a disorder-induced smoothening of the sharp features at the Fermi level in the samples.

The temperature dependence of the thermopower of heavy–fermion systems shows a wide variety of different features. In the trivalent cerium systems a sign reversal with a negative low temperature minimum is a common feature in concentrated systems. Recently Kim and Cox [41] discussed the possible realization of a two-channel Kondo impurity model in Ce^{3+} predicting a large negative thermopower in a cubic crystal symmetry and non-Fermi-liquid signatures in thermodynamic quantities. In dilute Cerium systems, however, a negative thermopower has never been observed. In recent measurements on $La_{0.9}Ce_{0.1}Cu_{2.2}Si_2$ [40] a clearly positive thermopower is observed which is in strikingly good qualitative agreement with our calculation (see single–impurity calculation of $S(T)$ in Fig. 4). For temperatures $T \geq T_K$ the lattice and the impurity thermopower calculated within our model are very similar since coherence no longer plays a role and the impurity concentration explicitly cancels in equation (26). On the other hand the thermopower sensitively measures the asymmetry of the scattering rate above and below the chemical potential. In our opinion the negative thermopower of $CeCu_2Si_2$, which is still not properly understood, points towards additional lattice effects not included in our model. Besides a possible influence of the band structure, non–local quasiparticle interactions, which are not contained in the local approximation, cause significant renomalizations of the one-particle properties. These interactions mediate short–range antiferromagnetic fluctuations whose correlation length can grow with decreasing temperature. Assuming a quantum critical point ($T_N \to 0$) the fluctuations can account for the observed non-Fermi-liquid behavior in $CeCu_2Si_2$ above the superconducting T_c [40].

With increasing valence instability a crossover to an overall positive thermopower with a second low temperature maximum is observed (see *e.g.* in $CeRu_2Si_2$ [42]). One possible reason for the negative component of the

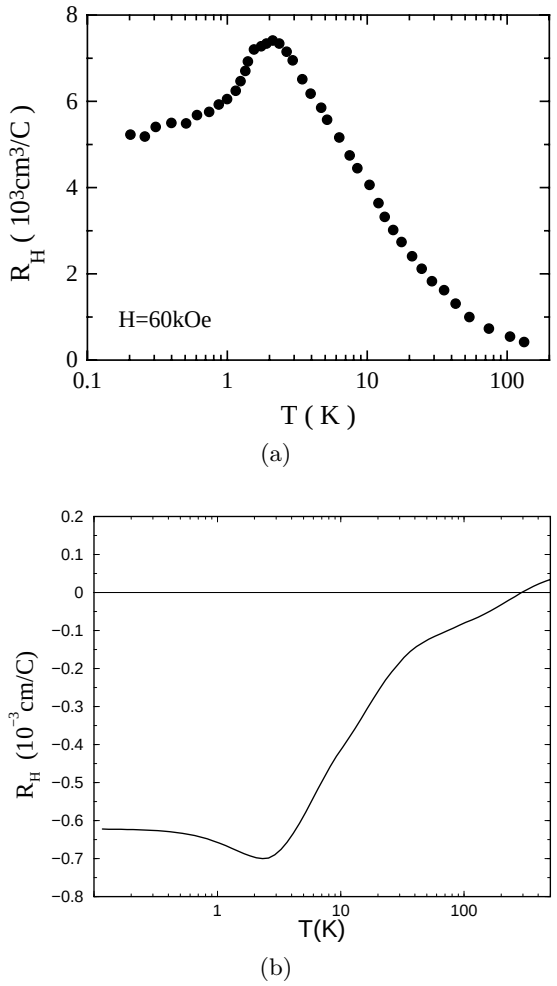

Fig. 5. Comparison of the Hall coefficient of $CeCu_2Si_2$ [45] (a) with the model calculations (b).

thermopower is given by intersite spin-interactions. Consequently, due to the onset of real charge fluctuations on the f-sites the negative part of the thermopower is suppressed [43]. Spin-spin interactions are not included in the calculation, so the qualitative feature with two maxima in the calculated thermopower might be more representative of systems like $CeRu_2Si_2$.

We conclude this section with some remarks concerning the Hall coefficient, depicted in Figure 5. In this case the discrepancies between the calculation and the experimental data are especially pronounced. $CeCu_2Si_2$ shows a skew–scattering behavior typical of all heavy-fermion systems and this is not reproduced by the calculation. On the other hand, the Hall coefficient can vary appreciably in magnitude and sign within a set of samples of the same heavy-fermion system. The intricate influence of inter–site spin interactions might be responsible for the strong deviations of the calculations from the experimental data. Nevertheless, the calculations predict in the Fermi-liquid regime a negative quadratic temperature dependence. With increasing temperature the skew-scattering part of the Hall coefficient increases and eventually overcompensates the negative Fermi-liquid contribution. As a result, a low–temperature minimum in the Hall coefficient develops. This was experimentally observed in several heavy-fermion systems and was discussed in more detail in [46].

4 Conclusions

The electronic transport properties of heavy-fermion systems were calculated on the basis of a semiphenomenological approach to the dynamical mean field theory in the limit of infinite local Coulomb repulsion augmented by crystal-field effects. The calculation is able to reproduce the qualitative features of the temperature-dependent resistivity, the magnetoresistivity and the thermoelectric power, as exemplified by a comparison with experimental data of $CeCu_2Si_2$ and $La_{0.9}Ce_{0.1}Cu_{2.2}Si_2$. The skew–scattering characteristic of the temperature dependent Hall coefficient could not be reproduced. Nevertheless, the lack of agreement between the experimental data and the calculation could presumably be traced back to secondary effects which are not included in our model. In particular, the disorder-induced suppression of coherent scattering in the resistivity and inter-site spin interactions, which might especially influence the thermoelectric power and the Hall coefficient, were not taken into account.

Within the scope of this approach an extension to include crystal–field excitations to magnetic singlet states can be easily accomplished by adding the respective resistivity or, more generally, the self–energy contributions of the singlet states as described by Cornut and Coqblin [12]. This permits the calculation of the transport properties of the uranium–based heavy–fermion systems, which tend to be in a $5f^2$–state [47].

A more sophisticated transport theory based on the Kubo formalism might be neccessary to account for the generally anisotropic band structure and probably an anisotropic hybridization. This might result in a more quantitative agreement between the experimental data and the calculated transport coefficients. However, in our opinion the consideration of non–local quasiparticle interactions is essential in order to account for the observed behavior of the thermopower and Hall coefficient. This is surely beyond the present approach and should be devoted to calculations based on a fully microscopic description of the electronic transport properties in heavy–fermion systems.

This work was supported by the Deutsche Forschungsgemeinschaft through SFB 252. Additionally, one of us (F.B.A.) was supported by the Deutsche Forschungsgemeinschaft, in part by the National Science Foundation under Grant No. PHY94-07194, and the US Department of Energy, Office of Basic Energy Science, Division of Materials Research. F.B.A. would like to thank the Institute for Theoretical Physics (ITP) in Santa Barbara, California, USA, for its hospitality where part of the work has been performed.

References

1. *e.g.* for a review, see: N. Grewe, F. Steglich, *Heavy Fermions* in *Handbook of the Physics and Chemistry of Rare Earths*, edited by K.A. Gschneidner Jr., L. Eyring (Elsevier, 1991), Vol. 14.
2. H. Keiter, J.C. Kimball, Int. J. Magn. **1**, 233 (1971); N. Grewe, H. Keiter, Phys. Rev. B **24**, 4420 (1981); H. Keiter, G. Morandi, Phys. Rep. **109**, 227 (1984).
3. K. Wilson, Rev. Mod. Phys. **47**, 773 (1975); N.E. Bickers, Rev. Mod. Phys. **127**, 845 (1987); P. Schlottmann, Physics Reports, **1&2**, 181 (1989); A.C. Hewson, *The Kondo Problem to Heavy Fermions* (Cambridge University Press, Cambridge, 1993).
4. Th. Pruschke, M. Jarrell, J.K. Freericks, Adv. Phys. **44**, 187 (1995).
5. A. Georges, G. Kotliar, W. Krauth, M.J. Rozenberg, Rev. Mod. Phys. **68**, 13 (1996).
6. N. Grewe, Th. Prusche, Z. Phys. B **60**, 311 (1985).
7. A.J. Millis, P. Lee, Phys. Rev. B **35**, 3394 (1987).
8. D.L. Cox, N. Grewe, Z. Phys. B **71**, 321 (1988).
9. A. Lorek, F. Anders, N. Grewe, Solid State Commun. **78**, 167 (1991).
10. Th. Pruschke, R. Bulla, M. Jarrell, Phys. Rev. B **61**, 12799 (2000).
11. S. Maekawa, S. Kashiba, M. Tachiki, S. Takahashi, J. Phys. Soc. Jpn **55**, 3194 (1986).
12. B. Cornut, B. Coqblin, Phys. Rev. B **5**, 4541 (1972); Y. Lassailly, A.K. Bhattacharjee, B. Coqblin, Phys. Rev. B **31**, 7424 (1985).
13. A.K. Bhattacharjee, B. Coqblin, M. Raki, L. Forro, C. Ayache, D. Schmitt, J. Phys. France **50**, 2781 (1989).
14. S.M.M. Evans, A.K. Bhattacharjee, B. Coqblin, Phys. Rev. B **45**, 7244 (1992); B.R. Trees, Phys. Rev. B **51**, 470 (1995).
15. M. Jarrell, Phys. Rev. B **51**, 7429 (1995).
16. R. Bulla, A.C. Hewson, Th. Pruschke, J. Phys. Cond. Matt. **10**, 836 (1998).
17. N. Grewe, Z. Phys. B **67**, 323 (1987); N. Grewe, Th. Pruschke, H. Keiter, Z. Phys. B **71**, 75 (1988).
18. P. Vorunganti, A. Golubentsev, S. John, Phys. Rev. B **45**, 13945 (1991).
19. K. Yamada, K. Yosida in *Theory of Heavy Fermions and Valence Fluctuations*, edited by T. Kasuya, T. Saso (Berlin, Springer, 1985), p. 184; K. Yamada, K. Yosida, Prog. Theor. Phys. **76**, 621 (1986).
20. F.B. Anders, D.L. Cox, Physica B **230-232**, 441 (1997).
21. Y. Kuramoto, *Theory of Heavy Fermions and Valence Fluctuations*, edited by T. Kasuya, T. Saso (Springer, Berlin, 1985), p. 152; C. I. Kim, Y. Kuramoto, T. Kasuya, Solid State Commun. **62**, 627 (1987); C.I. Kim, Y. Kuramoto, T. Kasuya, J. Phys. Soc. Jpn **59**, 2414 (1990).
22. For example a simple spin degenerate orbit with $U \rightarrow \infty$: $V^t(k,\uparrow) = (V(k),0)$, $V^t(k\ \downarrow) = (0,V(k))$ and $\sum_\sigma \underline{\underline{A}}(\mathbf{k}\sigma,z) = \begin{pmatrix} V(k)^2/(z-\epsilon_{\mathbf{k}\uparrow}) & 0 \\ 0 & V(k)^2/(z-\epsilon_{\mathbf{k}\downarrow}) \end{pmatrix}$.
23. V.I. Anisimov *et al.*, J. Phys. Cond. Matt. **9**, 7359 (1997).
24. M.B. Zölfl *et al.*, Phys. Rev. B **61**, 12810 (2000).
25. N. Grewe, Z. Phys. B **53**, 271 (1983)
26. Y. Nagaoka, Phys. Rev. A **138**, 1112 (1965); H. Suhl, Phys. Rev. A **138**, 515 (1965).
27. F.B. Anders, N. Grewe, Europhys. Lett. **26**, 551 (1994); F.B. Anders, J. Phys. Cond. Matt. **7**, 2801 (1995).
28. A.N. Tahvildar-Zadeh, M. Jarrell, J.K. Freericks, Phys. Rev. B **55**, R3332 (1997); A.N. Tahvildar-Zadeh, *et al.*, Phys. Rev. B **60**, 10782 (1999).
29. D.L. Cox, private communication.
30. Y. Onuki, T. Komatsubara, J. Magn. Magn. Mater. **63 & 64**, 281 (1987).
31. N. Grewe, B. Welslau, Solid State Commun. **66**, 1053 (1988).
32. B. Welslau, N. Grewe, Ann. Physik **1**, 214 (1992).
33. F.B. Anders, Phys. Rev. Lett. **83**, 4638 (1999).
34. H.J. Leder, G. Czycholl, in *Valence Fluctuations in Solids*, edited by F.M. Falicov, W. Hanke, M.B. Maple (North Holland Publishing Company, 1981), p. 237.
35. *e.g.* G. Rickayzen, *Green's Functions and Condensed Matter* (Academic Press, San Diego, 1980).
36. *e.g.* J.M. Ziman, *Principles of the Theory of Solids*, 2nd edn. (Cambridge University Press, London, 1972).
37. E.A. Goremychkin, R. Osborn, Phys. Rev. B **47**, 14280 (1993); E.A. Goremychkin, A.Yu. Muzychka, R. Osborn, Sov. Phys. JETP **83**, 738 (1996).
38. Y. Onuki, T. Hirai, T. Kumazawa, T. Komatsubara, Y. Oda, J. Phys. Soc. Jpn **56**, 1454 (1987).
39. E. Miranda, V. Dobrosavljević, G. Kotliar, Phys. Rev. Lett. **78**, 290 (1997).
40. F. Steglich, B. Buschinger, P. Gegenwart, M. Lohmann, R. Helfrich, C. Langhammer, P. Hellmann, L. Donnevert, S. Thomas, A. Link, C. Geibel, M. Lang, G. Sparn, W. Assmus, J. Phys. Cond. Matt. **8**, 9909 (1996).
41. T.S. Kim, D.L. Cox, Phys. Rev. Lett. **75**, 1622 (1996).
42. A. Amato, D. Jaccard, J. Sierro, P. Haen, P. Lejay, J. Flouquet, J. Low Temp. Phys. **77**, 195 (1989).
43. P. Link, D. Jaccard, P. Lejay, Physica B **225**, 207 (1996).
44. C.S. Garde, J. Ray, G. Chandra, Phys. Rev. B **45**, 7217 (1992).
45. F.G. Aliev, N.B. Brandt, V.V. Moshchalkov, M.K. Zalyalyutdinov, V. Kovachik, Sov. Phys. JETP **65**, 509 (1987).
46. M. Huth, J. Hessert, M. Jourdan, A. Kaldowski, H. Adrian, Phys. Rev. B **50**, 1309 (1994).
47. M. Huth, Ph.D. thesis, Darmstadt, Germany, 1995 (unpublished).